Simulation of Proton Exchange Membrane Fuel Cell by using ANSYS Fluent

Asifa Awan[1], Mahmood Saleem[1] and Abdul Basit[2]

[1]Institute of Chemical Engineering, University of the Punjab, Lahore, Pakistan
[2]Department of Chemical Engineering, University Technology PETRONAS, Malaysia

Email: msaleem.icet@pu.edu.pk

Abstract. Proton exchange membrane fuel cells (PEMFC) are attractive alternative source of electricity. The current study involves the computational fluid dynamics simulations of PEMFC under isothermal and non-isothermal conditions to investigate the performance of fuel cell. Effect of pressure and temperature on fuel cell performance is studied under non-isothermal conditions. PEMFC is modeled at 323 K and 1 atm under isothermal conditions whereas under non-isothermal conditions, the simulation is run on 353 K and 3 atm. The results show that the current density increases with increase in operating pressure of PEMFC and vice-versa with operating temperature.
Keywords. Simulation, proton exchange membrane, fuel cell, ANSYS Fluent

1. Introduction

Fuel cell converts chemical energy into electrical energy. It runs continuously until the reactants run out. The ever growing efficiency and very low emissions of fuel cells will ensure their commercial success in coming years [1]. PEMFC's operate at low temperatures (below 100 ^{o}C) which is easy to operate and handle. Recent research work on PEMFC is generally focused on its size, cost, performance and durability. Computer simulations are getting more attention of researchers as low cost option which produces reliable results.

PEMFC performance depends upon various factors like: Physical parameters (i.e. ref. current density, conc.), operating parameters (i.e. operating temperature, pressure), geometrical parameters, advanced parameters like contact resistance. Siegel C. et.al reviewed PEM fuel cell simulations performed on different softwares [2]. Researchers [3] validated PEMFC model for investigating convergence criteria. According to authors [4], incomplete and unreliable data is the main issue for obtaining correct tests.There is a lot of work going on flow fields to get better performance of PEMFC. Computational model developed for a 5 cm^2 fuel cell with serpentine and parallel flow fields are considered in experimentation and in modeling [5].

Simulation has been performed by modifying the design of flow field which decrease the pressure drop in PEMFC. Modifications are based on theory of injection engine to reduce pressure drop [6]. A comprehensive non isothermal, 3-D model is established to investigate the performance of PEMFC with straight and serpentine flow fields [7]. Aspect ratio of flow fields also has effect on fuel cell performance [8]. The local transport phenomena and cell performance is performed for parallel and integrated flow fields [9]. Effect of single (1-s), double (2-s) and triple (3-s) serpentine flow fields is also investigated. It is reported that effects of flow fields variations are negligible below 0.7 operating voltage [10]. A stepped flow field is proposed to improve cell performance [11]. Researchers made the comparison between the conventional straight gas flow channel and a novel wave-like channel [12]. Different shapes and lengths of parallel flow field affect cell performance [13].Water management is one of the main issues in PEM fuel cell [14].

Percolation theory was coupled with 3-D PEMFC model to investigate the effects of water flooding on gas diffusion layer [15]. Using different height and length tapered flow fields due to which velocity increases and water flooding does not produce, it also enhances rib-convection among

adjacent channels [16]. Muthukumar M et.al analyzed the effects of landing to channel (LXC) on the generation of power and current density [17]. Researchers [18] focus on the relation between flow velocity and optimum channel width. PEM permits only proton ions and PEM's activity depends upon the humidity on surface of membrane [19]. Researchers made the comparison between 3 phenomenological membrane models and the results indicates that springer model and Nguyen and white model over predict drying of the membrane while the fuller and new man model provides the best match with experimental data [20]. In present study the transport equations are used after [7].

Table 1. PEMFC Dimensions [7].

Cell dimensions	Units	Values
Gas channel length	mm	10
Height of gas channel	mm	1
Width of the gas channel	mm	1
Width of the cell	mm	2
Thickness of catalyst layer	mm	0.014
Thickness of gas diffusion layer	mm	0.0254
Thickness of current collector	mm	2.5
Thickness of membrane	mm	0.051
Overall cell height	mm	5.1295

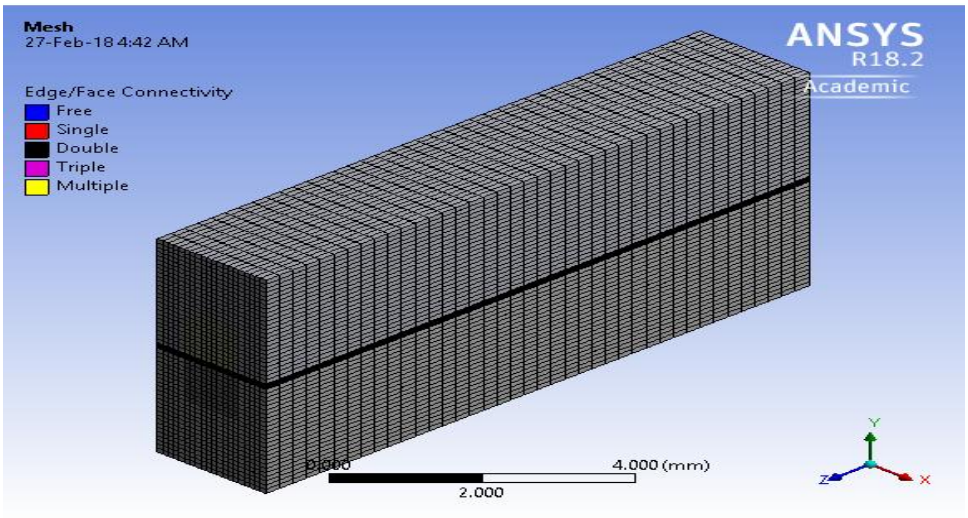

Figure 1. 3-D view of single channel PEMFC

2. Methodology

The simulated 3-D PEMFC consists of single straight channel shown in figure 1. The dimensions are given in table [1]. Boundary conditions and physical parameters used in the simulation are shown in tables 2 and 3 respectively. The model is developed with the following assumptions:

- Flow is laminar.
- Incompressible fluids.
- Steady state system exists.
- Inlet gases follow Ideal gas law.
- The catalyst layer, membrane and gas diffusion layer are Isotropic materials.

- For isothermal modeling temperature is constant.
- For non-isothermal modeling heat flux is constant.

Table 2. Boundary conditions (BC).

BC types	Location	Parameters	Non-Isothermal	Isothermal	Units
Velocity inlet	Inlet anode flow channel face	Velocity inlet	2	0.3	m/s
		Mass fraction of H_2	0.3	0.3	-
		Mass fraction of H_2O	0.7	0.7	-
	Inlet Cathode flow channel face	Velocity inlet	2	0.5	m/s
		Mass fraction of O_2	0.14	0.212	-
		Mass fraction of H_2O	0.2	.079	-
Pressure Outlet	Outlet anode flow channel face	Anode outlet gas pressure	0	0	Pa
		Temperature	Default	323	K
	Outlet cathode flow channel face	Cathode outlet gas pressure	0	0	Pa
		Temperature	Default	323	K
Wall	The terminal and upper anode current collector face	Specified electric potential	0 (only terminal)	0	Volts
	The terminal and lower cathode current collector face	Specified electric potential	0.5-0.9 (only terminal)	0.4-0.9	
	All Outer cell faces	Thermal condition constant Temperature	-	323	K
		Heat flux	0	-	

Table 3. Parameters values.

Parameters	**Isothermal**	**Non-isothermal**	**Units**
Cell operating temperature	323	353	K
Cell operating pressure	1	3	Atm
Open-circuit voltage	1.07	1.05	Volt
Anode Reference exchange current density	10,000	30	A/m^2
Cathode Reference exchange current density	20	0.004	A/m^2
CL Electric conductivity	Default	100	1/ohm-m
Current collector Electric conductivity	4000	Default	1/ohm-m
GDL Electric conductivity	300	Default	1/ohm-m
Anode exchange coefficient	1	0.5	-
Cathode exchange coefficient	1	2	-
Reference concentration of anode	1	0.04	-
Reference concentration of cathode	1	0.00086	
CL Porosity	0.112	0.6	-
GDL Porosity	0.6	0.6	-

ANSYS meshing is used to generate hexahedral mesh with 59200 cells whereas Fluent is used as a solver. Joule heating, electrochemistry and Butler-Volmer are used as model equations for

PEMFC simulation. SIMPLE algorithm is used for solving equations. The least square cell base is chosen under spatial discretization.

3. Results and Discussion

The simulation of single channel PEMFC is performed according to the condition given in tables 2 and 3. Results are presented in figure 2 and 3. The models are validated by using data of Lee Wang et.al. [21] and the results are in good agreement with the experimental data except for the low current density region under non-isothermal conditions and high current density region under isothermal conditions. As the redox reaction in the fuel cell increases, the current density also increases. At high current density, production of water increases in catalyst layer and gas diffusion layer (GDL), due to which effective porosity of catalyst layer and GDL decreases and material resistance increases. The assumption of the simulation that water is being produced in the form of mist does not remain valid due to this phenomenon at high current densities as the large quantities of liquid water fill the pores of catalyst and membrane, thereby increasing transport resistance [5].

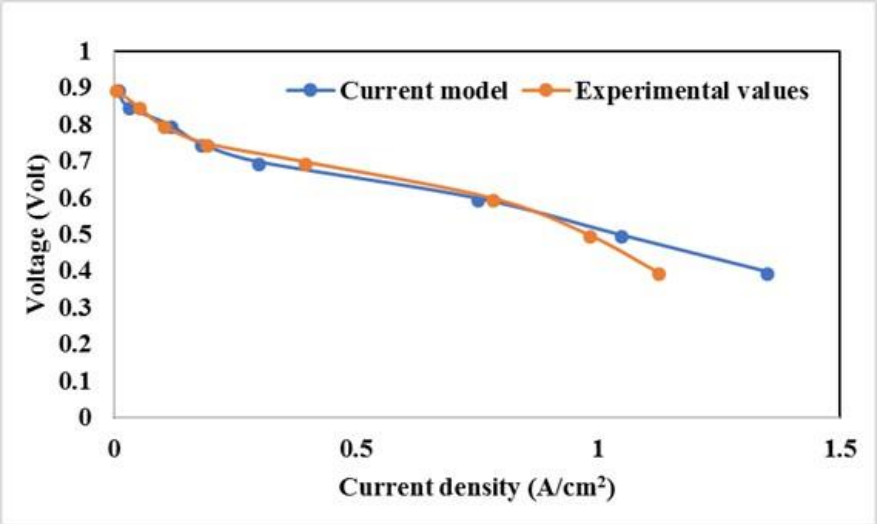

Figure 2. Comparison of simulation and experimental results under isothermal conditions.

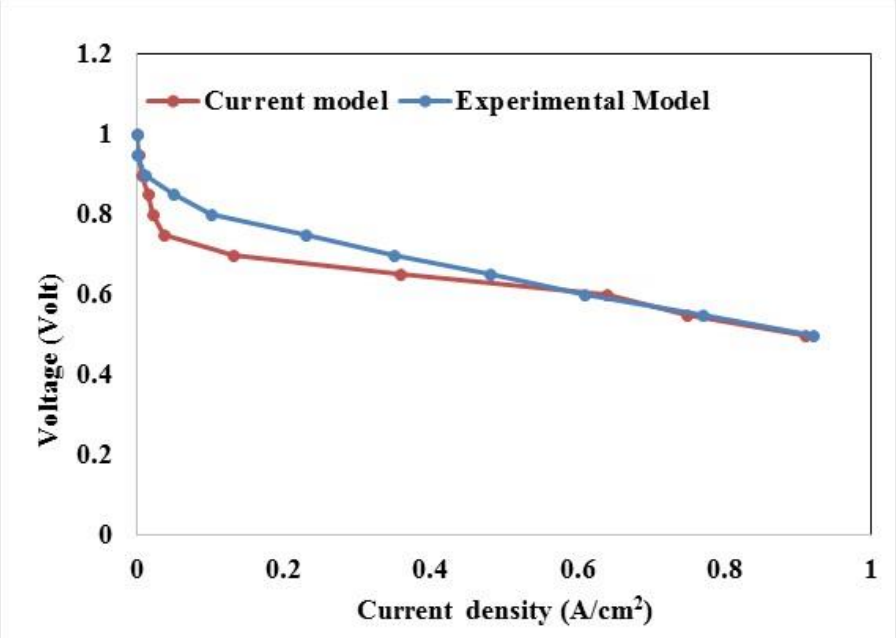

Figure 3. Comparison of simulation and experimental results under non-isothermal condition.

The most affecting reactant at higher current density is oxygen, as shown in figure 4 (a). The mass fraction of oxygen is very high in cathode channel at 353 K. Under the current collector, oxygen is more depleted in MEA region. This might be due to the limited oxygen diffusivity and also due to the difficulty of water removal in cathode side. As vapor saturation pressure depends on temperature, the relative humidity decreases with the increase in temperature. The membrane might be dehydrated thereby slowing the protonic ions permeation and leads to ohmic losses. Another reason of high mass fraction of oxygen might be slow protonic ions generation in membrane as compared to oxygen diffusion into GDL. On the other hand, it can be clearly seen that at high current density there is low change in hydrogen value as compared to oxygen as shown in figure 4 (b). Because hydrogen (small molecule) has better diffusivity than oxygen and it shows better transport at high current density even if the porosity is low. Usually there is no blockage at porous region of hydrogen side because flooding is not taking place on anode side. Pressure decreases from inlet to outlet as shown in pressure contours in figure 4(c). Temperature increases from inlet to outlet as shown in temperature contours in figure 4(d) due to reduction reaction and ohmic losses.

The current densities over-potential near the CCL/PEM interfaces are so big that the maximum current density generated in cathode region is produced on this interface. At this current density, starvation region is clearly shown in figure 5 under the current collector region; this might be due to oxygen diffusivity problem [22].

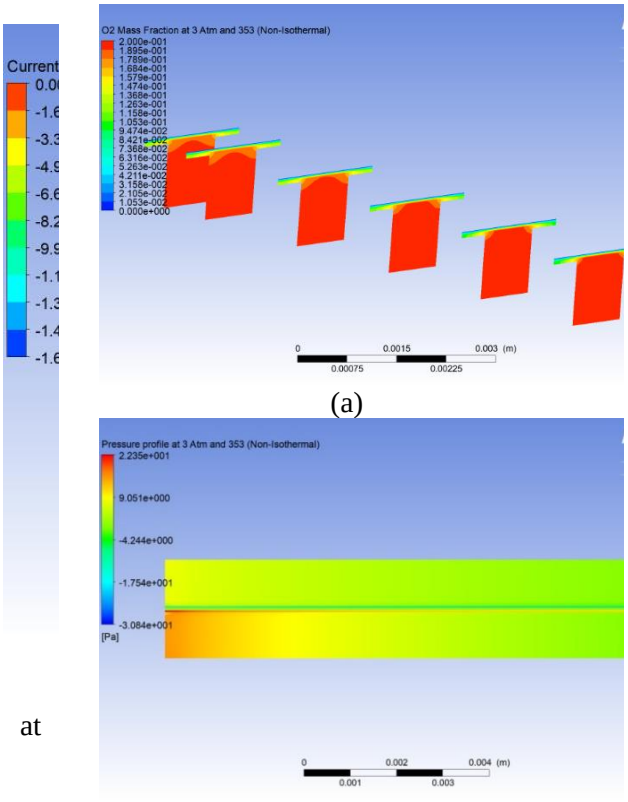

Figure 4. Mass fraction distribution under non-isothermal conditions at 0.6 volts for (a) O_2 (b) H_2 (c) Static pressure (d) Temperature.

at 0.6 volts non- isothermal.

Figure 5. Current Distribution

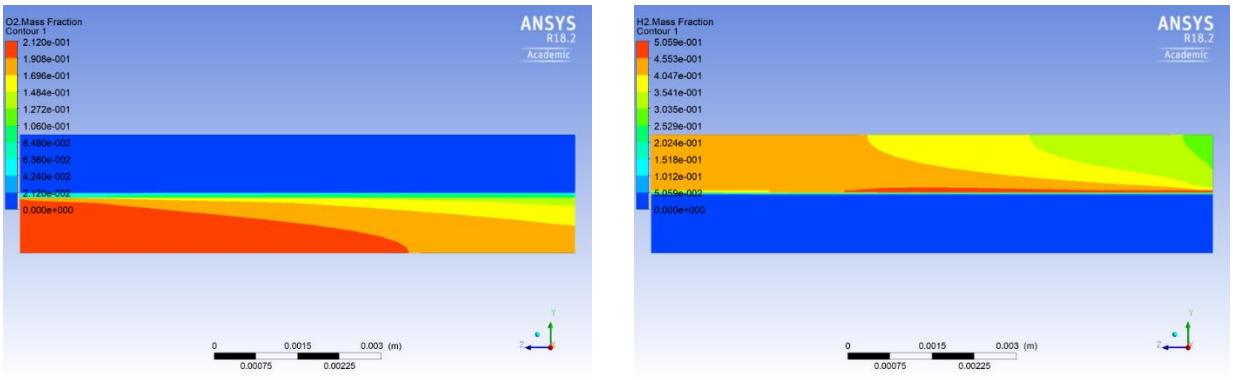

(a) (b)

Figure 6. Mass fraction distribution under isothermal conditions at 0.6 volts for (a) O_2 (b) H_2

Oxygen mass fraction decreases from inlet to outlet because oxygen is consumed in the reaction on its way to the outlet. Current density is greater at the hydrogen inlet as compared to oxygen inlet since the reaction starts at hydrogen inlet as shown in figure 6.

It is shown in figure 4 and figure 6 that no gases are present in MEA region of fuel cell. This means that at anode side, the hydrogen ions enter into the catalyst layer while on cathode side, oxygen ions enter into the catalyst layer instead of gas molecules [23].

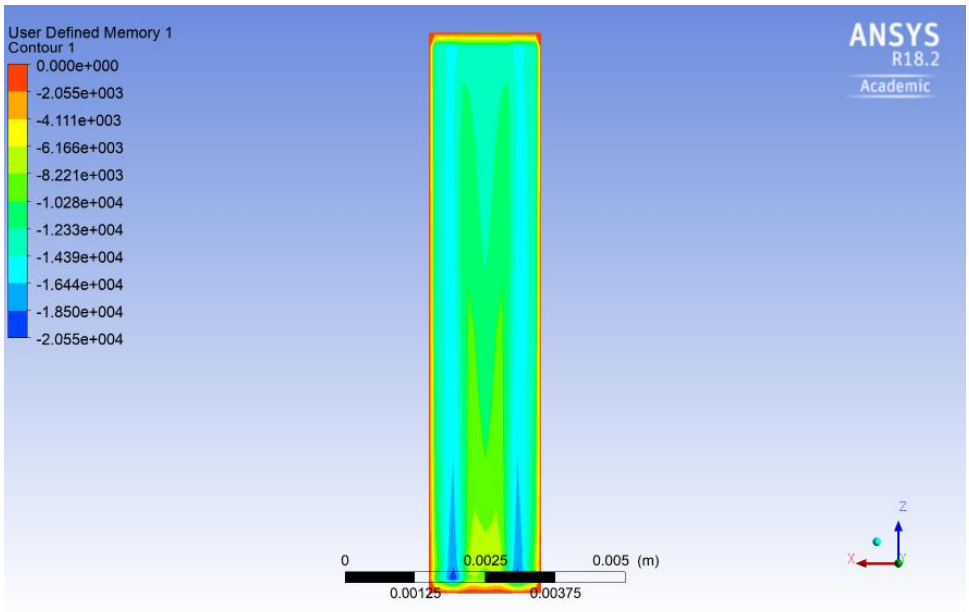

Figure 7. Current distribution at 0.6 volts (isothermal).

Current density value is low at collectors rib because there is depletion of oxygen in those region which is shown in figure 7. Drying of anode side might be major cause of decrease in cell performance. Multi-phase model should be used to observe this phenomenon in detail [5].

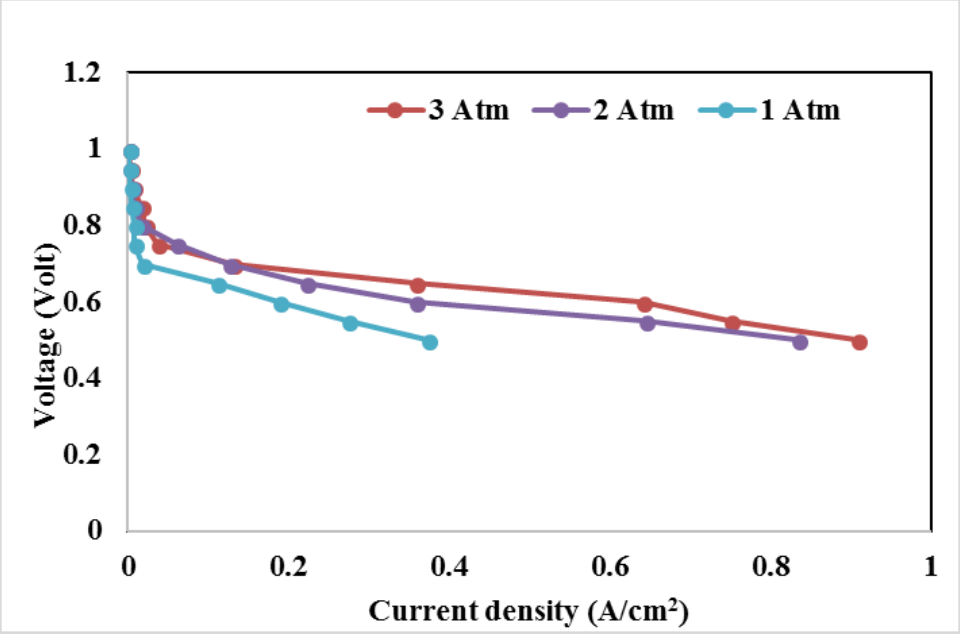

Figure 8. Effects of Pressure on voltage and current density at 253 K.

Polarization curves of different pressures at 353 K temperature are shown in figure 8. The pressures of both anode and cathode sides were kept the same. The performance of the fuel cell improves with the increase of pressure. The overall polarization curves shift positively as the pressure increases. With the increase in pressure, partial pressure of the reactant gases increases [21].

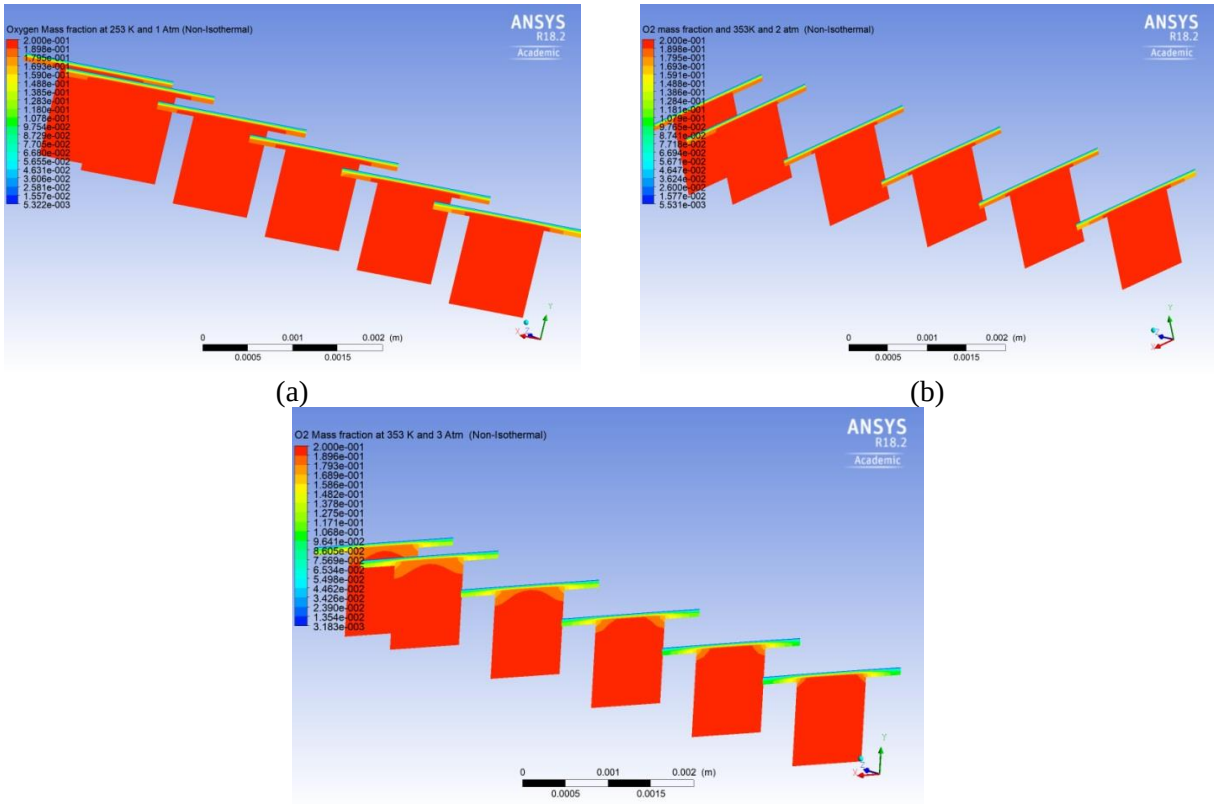

(a) (b)

(c)

Figure 9. Mass fraction of oxygen at (a) 1 atm (b) 2 atm (c) 3 atm.

The mass fraction of oxygen decreases in PEMFC as the operating pressure is increased as shown in figure 9. The decreased mass fraction is due to increase in reaction rate which is favored by increased operation pressure.

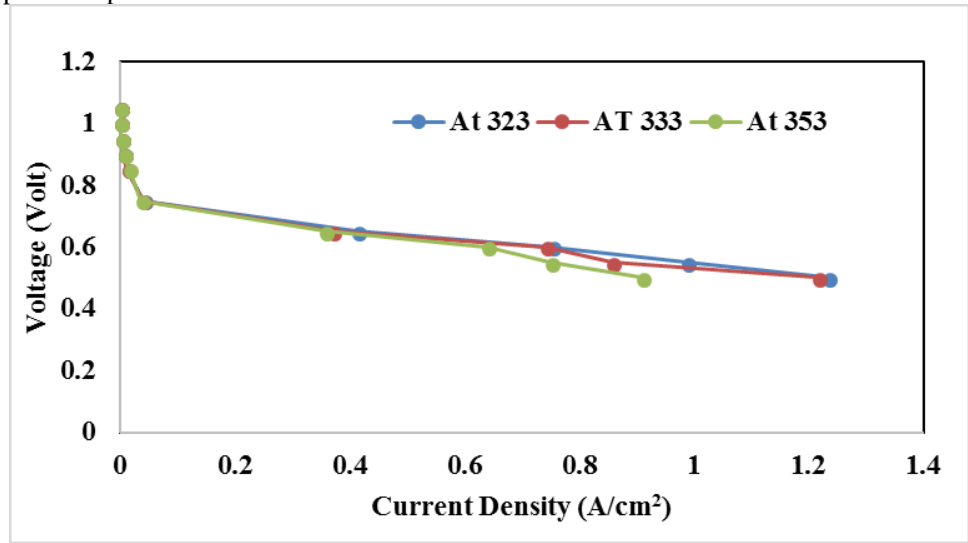

Figure 10. Effect of Temperature on voltage and current density.

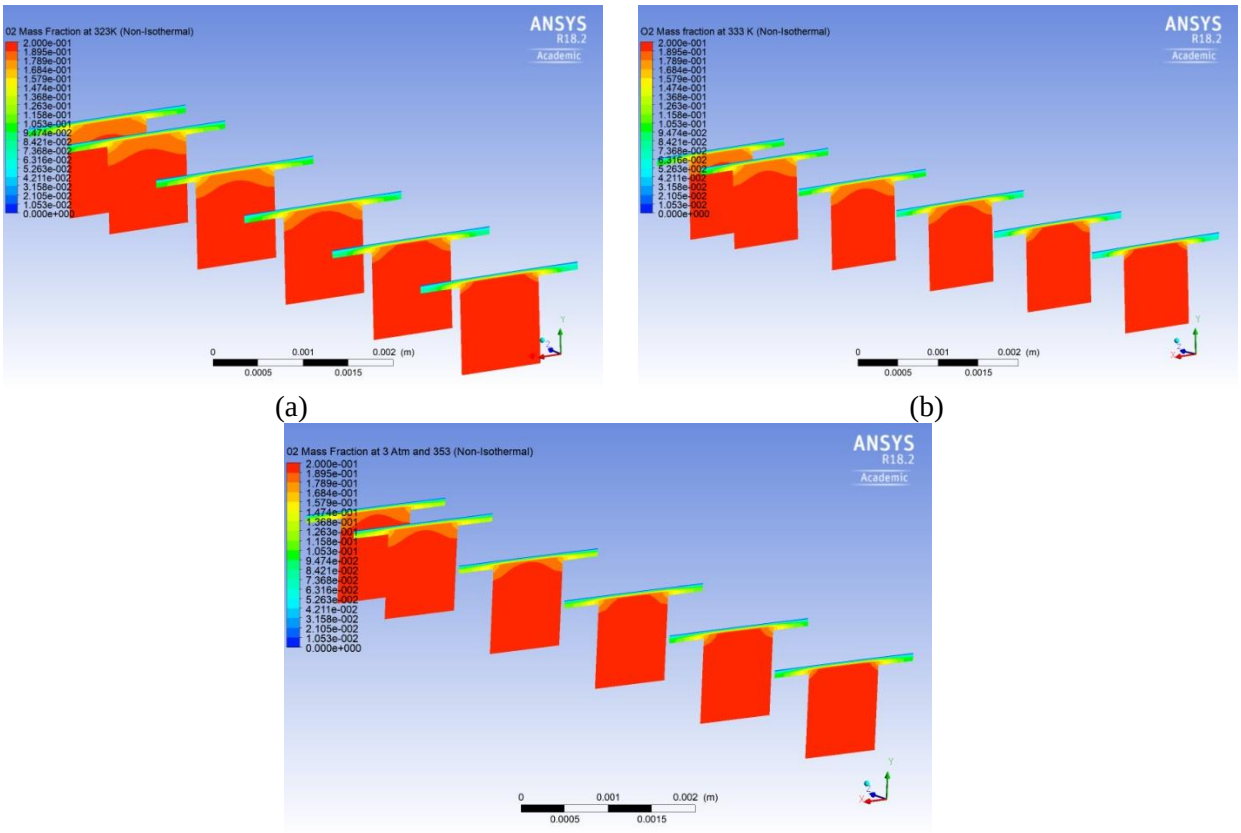

Figure 11. Mass Fraction of O_2 at 323K (a), 333K (b) and 353K (c).

Polarization curve at different temperatures are shown in figure 10. Oxygen mass fraction is shown in figure 11. Oxygen mass fraction distribution is often considered the criteria of fuel cell performance because the diffusivity of hydrogen is high as compared to oxygen. As the temperature is increased, humidification decreases and leaves the membrane less hydrated [24]. Oxygen mass fraction is slightly high at 353 K and 333 K as compared to 323K as shown in figure 11.

4. Conclusions

Simulation of single straight channel, proton exchange Membrane fuel cell is carried out under isothermal and non-isothermal conditions. Non-isothermal flow design is co current flow and isothermal model is counter flow design. It is observed that current was being produced at inlet of hydrogen. No oxygen and hydrogen molecules can enter into catalyst layer and membrane. Models predictions are compared with published experimental data which are in good agreement. The deviations observed might be due to single phase assumption in the study. Temperature and pressure are one of very important parameters which play main role in cell performance. The results show that cell performance under non-isothermal conditions is better at higher pressures.

List of Symbols

CL	Catalyst layer	i_a, i_c	Transfer current density for anode and cathode
GDL	Gas diffusion layer	i_c^{ref}	Ref. exchange current density per surface area Cathode
CC	Current collector	ζ_a	Specific active surface area at anode
F	Faraday constant	ζ_c	Specific active surface area at cathode
M	molecular weight (kg/mol)	i_a^{ref} , i_c^{ref}	Ref. exchange current density per surface area of Anode
ε	porosity	$\emptyset_{sol}$	Electric potential
ρ	density	$\emptyset_{mem}$	Protonic potential
$\vec{\mathbf{u}}$	velocity vector	σ_{sol}, σ_{mem}	Electrode conductivity, Ionic conductivity
$\vec{\boldsymbol{\tau}}$	shear tensor	λ_{eff}	Effective thermal conductivity in a porous media
μ	Viscosity	$\vec{J}_k$	diffusional mass flux vector of specie k
$\mathbf{k_i}$	Permeability of GDL and CL	λ_S	Thermal conductivity of solid porous media
$\vec{\boldsymbol{\tau}}_{\mathbf{eff}}$	Effective stress tensor	$\eta_{a,c}$	Over potential at anode and cathode
$\mathbf{h_k}$	Enthalpy of species k	$D_{k,j}^{eff}$	Effective diffusional coefficent
$\mathbf{Y_k}$	mass fraction y species	p_0	Reference pressure
T	Temperature	p	pressure
$\mathbf{T_0}$	Reference temperature		

References

[1] Barnett, B.M. and Teagan, W.P 1992 The role of fuel cells in our energy future Journal of Power Sources 37 15-31
[2] Siegel, C., 2008 Review of computational heat and mass transfer modeling in polymer-electrolyte-membrane (PEM) fuel cells Energy 33 1331–1352
[3] Arvay A, Ahmed A, Peng X-H and Kannan AM 2012 Feb Convergence criteria establishment for 3D simulation of proton exchange membrane fuel cell Int J Hydrog Energy 37 2482–9

[4] Bednarek T and Tsotridis G. 2017 Mar Issues associated with modelling of proton exchange membrane fuel cell by computational fluid dynamics J Power Sources 343 550–63
[5] Iranzo A, Muñoz M, Rosa F and Pino J. 2010 Oct Numerical model for the performance prediction of a PEM fuel cell Model results and experimental validation. Int J Hydrog Energy 35 11533–50
[6] Wilberforce T, El-Hassan Z, Khatib FN, Al Makky A, Mooney J and Barouaji A, et al. 2017 Oct Development of Bi-polar plate design of PEM fuel cell using CFD techniques Int J Hydrog Energy 42 25663–85
[7] Hashemi F, Rowshanzamir S and Rezakazemi M. 2012 Feb CFD simulation of PEM fuel cell performance: Effect of straight and serpentine flow fields Math Comput Model 55 1540–57
[8] Cooper NJ, Santamaria AD, Becton MK and Park JW. 2017 Mar Investigation of the performance improvement in decreasing aspect ratio interdigitated flow field PEMFCs Energy Convers Manag 136 307–17
[9] Wang X-D, Duan Y-Y, Yan W-M and Peng X-F. 2008 Jun Effects of flow channel geometry on cell performance for PEM fuel cells with parallel and interdigitated flow fields Electrochimica Acta 53 5334–43
[10] Velisala V and Srinivasulu GN. 2018 Mar Numerical Simulation and Experimental Comparison of Single, Double and Triple Serpentine Flow Channel Configuration on Performance of a PEM Fuel Cell Arab J Sci Eng. 43 1225–34
[11] Min C-H. 2009 Jan Performance of a proton exchange membrane fuel cell with a stepped flow field design J Power Sources 186 370–6
[12] Kuo J-K, Yen T-H and Chen C-K. 2008 Feb Three-dimensional numerical analysis of PEM fuel cells with straight and wave-like gas flow fields channels J Power Sources 177 96–103
[13] Barakat E, Ahmed K, Ahmed M, Abdel-Rahman AK and Ali AHH 2013 Int. Conf. & Exhibition on Clean Energy (Ottawa, Ontario, Canada) vol 1 p 268
[14] Le AD and Zhou B. 2008 Jul A general model of proton exchange membrane fuel cell J Power Sources 182 197–222
[15] Dawes JE, Hanspal NS, Family OA and Turan A. 2009 Jun Three-dimensional CFD modelling of PEM fuelcells: An investigation into effects of water flooding ChemEng Sci. 64 2781-94
[16] Wang C, Zhang Q, Lu J, Shen S, Yan X and Zhu F et al. 2017 Sep Effect of height/width-tapered flow fields on the cell performance of polymer electrolyte membrane fuel cells Int J Hydrog Energy 42 23107–17
[17] Muthukumar M, Karthikeyan P, Vairavel M, Loganathan C, Praveenkumar S and Kumar APS. 2014 Numerical Studies on PEM Fuel Cell with Different Landing to Channel Width of Flow Channel Procedia Eng. 97 1534–42
[18] ZareNezhad B and Sabzemeidani MM. 2015 Predicting the effect of cell geometry and fluid velocity on pem fuelcell performance by CFD simulation J Chem Technol Metall. 50 176–182
[19] Shimpalee S, Dutta S, Lee WK and Van Zee JW. 1999 Int Mechanical Engineering Congress & Exposition (Nashville, Tennessee, November 14 - 19, 1999) pp 367–374
[20] Kamarajugadda S and Mazumder S. 2008 Jul On the implementation of membrane models in computational fluid dynamics calculations of polymer electrolyte membrane fuel cells Comput Chem Eng. 32 1650–60
[21] Wang L. 2003 Nov A parametric study of PEM fuel cell performances Int J Hydrog Energy 28 1263–72
[22] Baca CM, Travis R and Bang M.2008 Mar Three-dimensional, single-phase, non-isothermal CFD model of a PEM fuel cell J Power Sources 178 269–81
[23] Cheddie DF and Munroe NDH. 2006 Sep Three dimensional modeling of high temperature PEM fuel cells J Power Sources 160 215–23
[24] Kazemi Esfeh H, Azarafza A and A. Hamid MK. 2017 On the computational fluid dynamics of PEM fuel cells (PEMFCs): an investigation on mesh independence analysis RSC Adv. 7 32893–902